VOL. 6, NO. 8, AUGUST 2011 ISSN 1819-6608
ARPN Journal of Engineering and Applied Sciences

www.arpnjournals.com

STUDY THE EFFECT OF FLOW BYPASS ON THE PERFORMANCE OF A SHROUDED LONGITUDINAL FIN ARRAY

Ahmed F. Khudheyer
Mechanical Engineering Department, al-Nahrain University, Baghdad, Iraq
E-Mail: ahyaja@yahoo.com,

ABSTRACT

Theoretical and experimental studies were carried out to investigate the effects of duct velocity, fin density and tip-to-shroud clearance on the flow bypass and its impact on the pressure drop across a longitudinal aluminum fin array and its thermal performance. The clearance was varied parametrically, stating with the fully shrouded case and variations of the channel height giving partially shrouded configuration of different clearance ratios were also carried out. The flow bypass was found to increase with increasing fin density and insensitive to the air flow rate. That effect of fin density decreased as the clearance increased. The calculated total pressure was greatly affected by fin density. For fully-shrouded fin array, with H_f /S equals to 8 and 12.75, the pressure drop increased by a factor of 4.3 and 20 of that with H_f /S equals to 3.4, respectively. The total pressure drop and the average convective heat transfer coefficients corresponding to the fully and partially shrouded fin array of H_f /S=3.4 were compared. Going from fully to partially shrouded one of the largest clearance ratio (C/H_f =0.89), the total pressure drop reduced by about 50%. For clearance ratios equal to 0.36, 0.56, and 0.89, the average heat transfer coefficients were reduced by about 12, 17, and 30 percent of those for the fully shrouded configuration at Re_D of about 3×10^3. That percentage reduction in heat transfer coefficients decreased with the increase of air flow rate.

Keywords: longitudinal fin arrays, thermal performance, fin density.

INTRODUCTION

Increasing power density of electronic equipment are requiring more effective thermal enhancement to maintain its operating temperatures at a satisfactory level. Despite its relatively poor thermal properties, air through the use of extended surfaces continuous to be used as a coolant for many electronic devices. Design of such surfaces takes the form of longitudinal fin arrays. If the air velocity through the gaps between fins is well approximated, the thermal performance of such fin arrays and pressure drop across them can be detected. Approximating the fin velocity based on the upstream flow rate in the enclosure is difficult, unless the fin array is fully shrouded, which is not practical. In ducting fin arrays, the approach flow redistribute itself and at least a portion of it will take the path of least resistance and bypass the fin array. The performance of such fin arrays is adversely affected by this flow bypass.

Recently, the studies on heat sink design for forced convection have been conducted. Bejan and Sciubba [1992] have predicted the optimal fin spacing for maximum heat transfer from a package of parallel plates that is cooled by forced convection. Knight *et al*. [1992] have developed fin optimization method for heat sink with micro channels by iterative solution of nonlinear equations for Reynolds number, friction factor, Nusselt number, fin length, and pumping power. Since the surrounding flow field of fin arrays is actually bypass flow over fins, bypass effect should be taken into account.

The effect of flow bypass on the performance of longitudinal fin arrays has been reported by several workers. Sparrow *et al*. [1978], Sparrow and Beckley [1981], and Sparrow and Kadle [1986] investigated the effect of tip clearance on thermal performance of longitudinal plate fin heat sink. It is reported that the ratio of heat transfer coefficient with and without clearance, to be strongly affected by the tip clearance to fin height ratio, and to be independent of air flow rate and fin height. Experimental results of Butter baugh and Kang [1995] showed that the thermal resistance is strongly correlated with the pressure drop across the heat sink, and appearing to be independent of the amount of bypass.

Writz *et al*. [1994] studied the effects of flow bypass on the performance of longitudinal heat sinks in ducted flow. It is reported that the values of flow bypass was found up to 60% and its effect was to reduce the overall heat transfer rate. Their study also showed that the design of fin arrays can be optimized for a given flow conditions and shroud configuration. Lee [1995] has analyzed the relationship between the fin geometry and the pressure drop across the fin array taking into account flow bypass from the hydrodynamic analysis and developed an analytical model for optimizing the thermal performance of longitudinal fin arrays in ducted flow.

Thermal characteristics of straight channel longitudinal fin heat sink under forced air cooling were experimentally and numerically investigated using CFD code by Adam and Izundu [1997]. It is reported that much of the augmentation in the heat transfer rates with the heat sink is due to the increased surface area. However, as observed by Writz *et al*. [1994], much of the gain in overall heat transfer rate is offset by the reduction in heat transfer coefficients due to the flow bypass effect which was more pronounced at lower approach flow rates.

Suzana *et al*. [2000] investigated the effects of fin density, air flow rate, and clearance area ratio on flow bypass and its impact on the thermal performance of the heat sink using CFD software. It is concluded that the flow

bypass is increased with the increasing fin density and clearance, while remaining insensitive to inlet duct velocity.

Azar and Tavassoli [2003] studied the effect of heat sink dimensions and the number of fins on its thermal performance. It is reported that the selection of heat sink depends not only on its thermal resistance, but also on the number of fins it has and how it is coupled to the board. Simons [2004] has estimated the air flow that actually passes through the fin passages of a ducted heat sink in the presence of flow bypass and investigated the effect of this flow bypass on its thermal performance. It is reported that the flow bypass has a substantial effect on thermal performance of heat sink, and that effect can significantly increase its thermal resistance as the number of fins increases.

Most of the experimental data collected from the previous studies in the above literature did not take the air flow leakage as well as the distribution of air flow through the duct into consideration. An adequate characterization of the thermal performance of such arrays requires a vast amount of data. More experimental work on them and with varying flow regimes is needed. The aim of the present study is to analytically and experimentally investigate the effect of air flow rate, fin density and tip-to-shroud clearance on flow bypass and its impact on the performance of a ducted longitudinal fin array.
Experimental Investigations

EXPERIMENTAL INVESTIGATIONS

Experimental setup

A wind tunnel is used to investigate the performance of the tested fin array. A schematic of this experimental setup is shown in Figure-1. It mainly consists of the test section, the power supplies, the flow rate, pressure and temperature measurement devices, a control gate, and the fan. An entry length for the tunnel is made from wood with enough length to assure a uniform flow upstream of the test section for inlet velocities ranging from 1m/s up to 20 m/s.

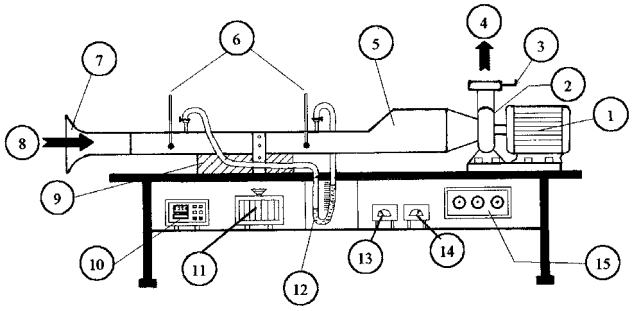

Figure-1. Test rig.

1- Electric motor, 2- Suction air blower, 3- Air flow control gate, 4- Air stream out, 5- Wooden duct, 6- Temperature probes, 7- Bell mouth, 8- Air in, 9- Test section, 10- Digital temperature recorder, 11-Autotransformer, 12- Manometer, 13- Voltmeter, 14- Ammeter, 15- Blower switchboard.

Test section components and configurations

For easy description of the experimental apparatus, reference may be made to Figure-2, which shows a view of the test section and a cross section of the ducted fin array assembly used in carrying out the experiments when fully shrouded. The wooden test section dimensions of 500×107mm with adjustable top allow accommodating the tested fin array. It includes an array of seven parallel longitudinal fins, a heated base plate, and a wooden shroud with adjustable top that can be moved up and down to change the amount of clearance between itself and the fin tips. The entire array can be easily mounted among the test section with the assurance of good thermal contact and to expose the fins to a nearly uniform air flow as can be reviewed in Elshafei and El-Negiry [2003].

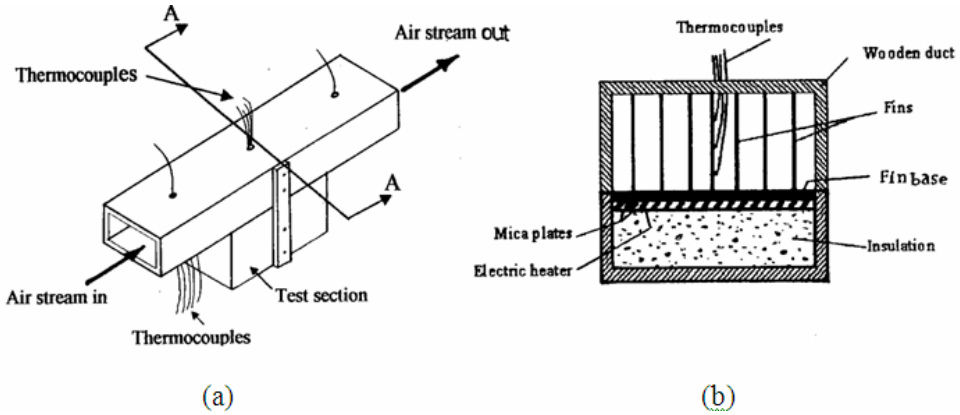

Figure-2. Test Section, (a) view of the test section, (b) cross sectional view at AA.

The fin/base plate assembly is fabricated from aluminum for its high thermal conductivity and low emissivity. An electrical resistance wire, which served to heat the fin array is sandwiched between two mica sheets and placed in contact underneath of the base plate and all the fin array assembly is then fitted into a wooden box filled with polystyrene insulation. The heat source is completely insulated on all sides in order to direct all heat to the fin array.

The closure of the fin gaps flow passages surrounded by an insulated U-shaped cross section wooden shroud with adjustable top, is attached to the fin array base plate at its outboard edges and sealed. This helps to minimize heat loss by conduction from the base plate to the shroud and prevent air leakage. The entire test section is insulated with glass wool sheet to minimize the heat loss.

As illustrated in Figure-2(b), the assembly of the tested fin array when fully shrouded and of 7 longitudinal fins with 6 parallel flow passages bounded by half width fin spacing between the end side fins and the shroud.

The wind tunnel is run in suction mode. Air is drawn from the laboratory through its developing length, and then passed a calibrated velocity meter into the test section. From there, the air is sucked through a rectangular cross section duct by a centrifugal fan followed by a control air flow gate.

Heating process and instrumentation

The electric power is supplied to the heater by a regulated AC source via an autotransformer to control the voltage. The voltage settings are guided by the readings of thermocouples, and both the voltage drop and the current are measured by Voltmeter and Ammeter respectively.

Nine T-type thermocouples, 0.5 mm diameter, are glued onto to the base of the fin array, in nine 1.5 mm diameter drilled holes in the bottom surface of the base plate. Another six thermocouples are positioned along the longitudinal length of the middle fin, three at the mid half of its height and the other three at its tip. The bulk air temperature is detected by averaging of the readings of two thermocouples inserted upstream and that of another two thermocouples inserted downstream of the test section respectively. Temperatures are recorded by connecting the ends of all thermocouples via a selector switch to a 6 channels digital temperature recorder of 0.1 $^{\circ}$C resolution and with an accuracy of $\pm$ 0.5 $^{\circ}$C.

The air flow rate is controlled by the graduated gate located at the wind tunnel exit. A calibrated digital hot wire anemometer with a range of 0.2-20 m/s, a resolution of 0.1 m/s, , and an accuracy of $\pm$ (1%+ 1d) full scale respectively is used to measure the average velocity of entering air with the help of a traversing mechanism located 150 mm ahead of the test section. Two static pressure taps are located 100 mm ahead and down stream of the test section and connected to a U-tube water manometer for the measurements of the pressure drop across the fin array assembly.

The test matrix

The ducted fin array assembly is shown in Figure-3. The clearance between the fin tips and the shroud which is represented by the top of the housing case is existed in practice such as in cooling of electronic components. When a clearance is present, the longitudinal flow tends to leak out of the fin passages where the flow resistance is low. The velocity distribution becomes more complex than for the no-clearance, as well as the heat transfer process.

In the present investigation, the height of the fins is held constant and the clearance between fin tips and the top of the test section can be varied by wooden smooth spacers with variable thickness that can be placed between the walls of the duct and the wooden shroud. The dimensional values of the fin array assembly used in the study are summarized in Table-1.

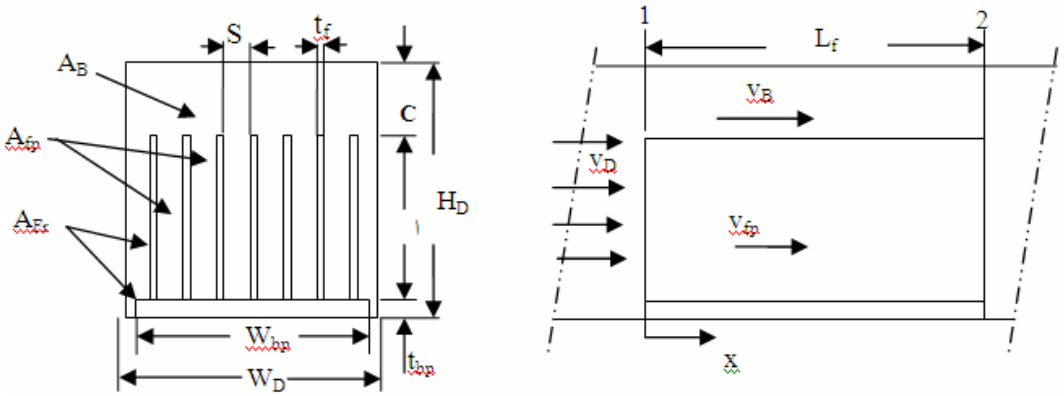

Figure-3. Ducted fin array and by pass flow geometry.

Table-1. Geometrical parameters of the tested fin array.

Parameter	Range modeled
Array material, Aluminum	k_f =237W/m.K
Number of fins, N_f	7
Base plate thickness, t_{bp}	3 mm
Bas plate, fin array width, W_{bp}	108 mm
Base plate length, L_{bp}	225 mm
Fin length, L_f	225 mm
Fin height, H_f	51 mm
Fin thickness, t_f	2 mm
Fin spacing, S	15 mm
Duct width, W_D	125 mm
Clearance, C	0,11.4,18.7, 28.6, 45.4 mm
Clearance ratio, C/H_f	0, 0.22, 0.36, 0.56, 0.89
Clearance space ratio, C/S	0, 0.76, 1.25, 1.9, 3.0
Duct height, H_D	51,62.4,69.7,79.6,96.4 mm

Heat transfer and pressure drop results are parameterized by conventional rectangular duct Reynolds number, defined as

$$\mathrm{Re}=\frac{v_D\, D_h}{\nu} \tag{1}$$

Where v_D is the duct air velocity upstream of the fin array and D_h is the hydraulic diameter of the fin array, given by

$$D_h=\frac{4A_F}{p} \tag{2}$$

Where A_F is the free flow area and p is the wetted perimeter of the whole fin array assembly, expressed as

$$A_F=\left(W_D-N_f\, t_f\right)H_f+W_D\, C-W_{bp}\, t_{bp} \tag{3}$$

$$p=2\left[\left(N_f+1\right)H_f+C+W_D\right] \tag{4}$$

The fin array was installed in its position inside the test section and tested for two different power inputs, 75 W, and 100 W, at various air flow rates in terms of Reynolds number.

To attain a steady state condition, the system was initially run for about two to three hour until constant values of the recorded temperatures for both the bulk air and the array surface were observed.

Bypass flow and pressure drop analysis

The tested fin array is installed in the test section within the rectangular cross sectional duct as shown in Figure-3. There will be a certain amount of flow bypasses and the velocity through the fin passages is different from the duct velocity approaching the fin array. The amount of bypass flow is related to the cross section geometry and the pressure drop across the fin array passages.

Considering the geometry shown in Figure-3, and applying momentum and mass balances over the control surfaces 1 and 2, the total pressure drop across the fin array as well as the by pass passages, Δp_t which is mainly consists of the pressure drop across the each passage due to friction and that due to the entrance and exit effects. This pressure drop is given by

$$\Delta P_t=\Delta P_{fp_f}+\frac{1}{2}K_{fp\,en}\rho v_{fp}{}^2+\frac{1}{2}K_{fp\,ex}\rho v_{fp}{}^2 \tag{5}$$

$$\Delta P_t=\Delta P_{B_f}+\frac{1}{2}K_{B_{en}}\rho v_B{}^2+\frac{1}{2}K_{B_{ex}}\rho v_B{}^2 \tag{6}$$

where ΔP_{fp_f} and $\Delta P_{B\,f}$ are the pressure drop across the fin array and by pass passages due to friction, and K_{en}, K_{ex} are the entrance and exit loss coefficients for both the fin array and by pass passages geometries respectively. These coefficients [Kays and London, 1984] are given by

$$K_{fp\,en}=0.42\left(\frac{A_{fp}}{A_D}\right)^2 \tag{7}$$

$$K_{fp\,ex}=\left(1-\left(\frac{A_{fp}}{A_D}\right)^2\right)^2 \tag{8}$$

$$K_{B\,en}=0.42\left(\frac{A_B}{A_D}\right)^2 \tag{9}$$

and

$$K_{B\,ex}=\left(1-\left(\frac{A_B}{A_D}\right)^2\right)^2 \tag{10}$$

Substituting equation (5) into equation (6) gives

$$v_B{}^2=\frac{\dfrac{f_{fp}L_{fp}}{D_{h_{fp}}}+K_{fp_{en}}+K_{fp_{ex}}}{\dfrac{f_BL_B}{D_{h_B}}+K_{B_{en}}+K_{B_{ex}}}v_{fp}{}^2 \tag{11}$$

Applying the continuity equation across the control surfaces, thus

$$v_B=\frac{v_D\, A_D-v_{fp}\, A_{fp}}{A_B} \tag{12}$$

where A_D is the duct cross sectional area approaching the fin array $(W_D \times H_D)$, expressed as

$$A_D = A_B + A_{fp} + A_{Fr} \quad (13)$$

A_B is the flow by pass area $(W_D \times C)$; A_{fp} is the flow area between fin array passages $\left(W_D - N_f t_f\right)H_f$, and A_{Fr} $(N_f H_f t_f + W_{bp} t_{bp})$ is the frontal area of the fin array.

Substituting equation (12) into equation (11), the flow velocity through the fin array passages (v_{fp}) can be described as a function of the duct flow velocity approaching the fin array (v_D) as follows

$$v_{fp} = \frac{-b \pm \sqrt{b^2 - 4ac}}{2a} \quad (14)$$

where

$$a = \left(\frac{A_{fp}}{A_B}\right)^2 - \frac{\frac{f_{fp} L_{fp}}{D_{h_{fp}}} + K_{fp_{en}} + K_{fp_{ex}}}{\frac{f_B L_B}{D_{h_B}} + K_{B_{en}} + K_{B_{ex}}},$$

$$b = \frac{-2 A_D A_{fp} v_D}{A_B{}^2},\ c = \left(\frac{A_D}{A_B}\right)^2 v_D{}^2,$$

$D_{h_{fp}} = \left(\frac{4\left(W_D - N_f t_f\right)H_f}{N_f\left(2H_f + S + t_f\right)}\right)$, and D_{h_B} is equals to $\left(\frac{2W_D \times C}{W_D + C}\right)$ are the hydraulic diameters of the fin array and the bypass passages, respectively.

The values of v_{fp} can be determined from equation (14), substituting the value of the duct velocity (v_D) with the assumption of preliminary values for the friction coefficients for both the fin array and by pass passages as a fully turbulent flow. The obtained value of v_{fp} is then recalculated through an iteration process using a correlation for the coefficient of friction [Hodge, 1990] described as

$$f = \frac{0.25}{\left[\log_{10}\left(\frac{\varepsilon}{D_h} + \frac{5.74}{\mathrm{Re}^{0.9}}\right)\right]^2} \quad (15)$$

The total pressure drop across the fin array is finally determined from equation (5) and compared with its measured values from the experiments.

As can be noticed in Figure-3, part of the incoming flow would bypass the fin array and is dependent on the amount of tip-to-shroud clearance, C. The flow by pass factor may be defined as the ratio of the bypassed flow rate and that actually passing through the fin array when it is fully shrouded. According to this definition, the flow by pass factor is expressed as

$$BF = \frac{\dot{V_B}}{\dot{V_D}} = 1 - \frac{v_{fp} A_{fp}}{v_D A_D} \quad (16)$$

Heat transfer analysis

Air flow with a uniform velocity, v_D and with a bulk temperature, T_∞ is flowing through the ducted constant heat flux heated fin array base. The part of the wooden test section containing the fin array assembly is wrapped with thick glass wool sheet insulation so that the rate of heat loss to the surroundings is so small and can be ignored. The rate of heat dissipation from the fin array and its base plate surfaces to the flowing through air is mainly by conduction and convection, given by

$$Q = Q_{in} - Q_L \quad (17)$$

Where Q_{in} is the rate of power input used to heat up the fin array base plate and Q_L is the rate of heat loss to the surroundings, which is neglected. Taking into account the effect of variation of the fin surface temperature along its height, the fin efficiency is introduced and Q can be described as

$$Q = h_{av}\, A_s \left(T_{bP} - T_\infty\right) \quad (18)$$

where A_s is the total surface area of the fin array assembly, given by

$$A_s = L_f \left[\left(W_{bp} - N_f t_f\right) + \eta_f\, N_f \left(2H_f + t_f\right)\right] \quad (19)$$

The fin efficiency, η_f for one dimensional heat flow with the presence of tip-to- shroud clearance can be expressed as

$$\eta_f = \frac{\tanh m H_{fe}}{m H_{fe}} \quad (20)$$

where

$$m = \sqrt{\frac{2 h_{av}}{k_f t_f}} \quad (21)$$

and H_{fe} is equal to $H_f + t_f/2$ in the presence of tip-to-shroud clearance and is reduced to H_f for fully shrouded fin array.

The average heat transfer coefficient h_{av} is calculated from Eq.18 by iteration with the help of experimental data, and presented in a dimensionless form as an average Nu, given by

$$\mathrm{Nu} = \frac{h_{av} D_h}{k_a} \quad (22)$$

The thermal conductivity of fin material is evaluated at the average of the fin surface temperature and

that for the air is evaluated at the average temperature of entering and leaving air to/from the fin array [Kakac *et al*., 1987].

RESULTS AND DISCUSSIONS

Flow bypass and pressure drop

The computed values of bypass factor for small, moderate and large clearance are shown in Figure-4. For a specific configuration, it is seen that the bypass factor slightly decreases with the increase of Reynolds number. In the mean time, the by bypass factor increases significantly from about 15% for a clearance ratio (C/H_f) of *0.22* up to *52%* for a clearance ratio of *0.89*. The flow bypass arises due to the presence of fins, obstructing the air flow and is greatly affected by the fin density as can be seen in Figure-5. Increasing fin density resulted in an increase in the bypass factor, and the percentage increase in its values is dependent on the amount of tip-to-shroud clearance. At a value for Reynolds number of about *12500*, and with clearance ratio of *0.22*, the %age increase in bypass factor for H_f/S equals to *8* and *12.75* related to that of H_f/S equals to 3.*4* is *23* and *61%*, while with a clearance ratio of 0.56, the %age increase in its value decreases to *16* and *36%* respectively. This is attributed to the fluid flow behavior with denser fin array and large clearance ratio, the air tends to flow into the clearance passage from the top of the fin array avoiding the fin passages of higher flow resistance generated by increased frictional losses and the increased acceleration due to change in cross section at the entrance of the fin array.

The variation of the calculated total pressure drop across the fully-shrouded fin array with different fin density against Reynolds number is shown in Figure-6. It is noticed that for all configurations, the pressure drop increases parabolically with Reynolds number. It is also seen that as the fin array becomes denser, the pressure drop increases significantly. At a certain value of Reynolds number, the pressure drop across an array of H_f/S equals to *8* and *12.75* increases by a factor of about 4 and 20 with respect to that of H_f/S equals to *3.4*, respectively.

The effect of fin spacing on the calculated pressure drop across the fin array with small and moderate clearance within the tested rang of Reynolds number is dissipated in Figure-7. It is observed that the pressure drop decreases with increasing tip-to-shroud clearance for all H_f/S values as well as the discrepancies between their pressure drop values. As discussed above, with larger clearance a greater amount of air is bypassed the fin array, reducing the air flow through its passages which causes lower values of pressure drop across it.

The effect of tip-to-shroud clearance on the calculated pressure drop across the experimentally tested fin array (N_f *=7,* H_f/S*=3.4*) is shown in Figures 8 and 9. The first of these shows the variation of the frictional component of the pressure drop with the variation of mass flow rates, while the second is for the total pressure drop across the fin array assembly including both the entrance and exit losses. The parabolic dependence of the pressure drop on the velocity is obvious for all configurations. As seen in Figure-8, the maximum frictional component of about *154 Pa* at the highest value of Reynolds number for fully shrouded fin array, nearly 4 times the frictional component of the configuration with largest clearance, and about 1.3 times at the lowest value of Reynolds number. Meanwhile, as can be noticed in Figure-9, the total pressure drop of about *450 Pa* at the highest Reynolds number for fully shrouded fin array, nearly three times the total pressure drop for that configuration of largest tip-to-shroud clearance, and this factor reduces to about *1.2* at the lowest Reynolds number.

A comparison of measured and computed total pressure drop across the experimentally tested fin array of different configurations is shown in Figure-10. A good agreement between the experimental data and the computed one is obtained. The differences between the measured data and the calculated data are relatively small and may be attributed to the lack of instrumentation and the values of the loss coefficients used in calculations.

Thermal performance of the tested fin array

Power input. The effect of power input on the heat transfer results is presented in Figure-11 for partially shrouded fin array with the largest clearance ratio *(C/H_f =0.89)*. For a specific configuration and with constant power input, the average heat transfer coefficient clearly increases with the increase of Reynolds number. The effect of changing power input on heat transfer is relatively small, especially at high values of Reynolds number. This conclusion agrees with the reported results by Suzana *et al*. [2000] and Elshafei and Elnigery [2003] for a fully shrouded fin array.

The impact of tip-to-shroud clearance on thermal performance of the tested fin array *(N_f =7, C/S=3.4)* heated with constant heat flux of *100 W* will be presented in the coming section.

Tip to shroud clearance. For fully and partially shrouded fin array configurations, the variations of the average heat transfer coefficient and the measured total pressure drop across the fin array with Reynolds number, Re_D are shown in Figures 12 and 13. Each graph contains five sets of data parameterized by two clearance ratios, C/H_f *of 0, 0.22, 0.36, 0.56, 0.89,* and *C/S of 0, 0.76, 1.25, 1.9* and *3.0.* Figure-12 shows as previously discussed that for a specific configuration, the Nusselt number increases with the increase of Reynolds number. At a given Reynolds number, the Nusselt number for partially shrouded fin array compared to that of fully shrouded, decreases significantly as the clearance ratio increases, expect that of *C/S* equals to *0.76*. This configuration offers higher values of Nusselt number for all values of Reynolds number above 7000. This may be attributed to the gain in the rate of heat transfer due to the promoted turbulence in that clearance gap (*C/S*) more than the degradation resulted from the bypassed air accompanied with that value of the clearance. It is also noticed that the effect of bypass on the average heat transfer coefficient diminishes

with the increase of Reynolds number. This agrees with the reported results of Adam and Izundu [1997].

As previously explained, the parabolic dependence of the measured total pressure drop on the flow velocity is also seen for all fin array configurations as seen in Figure-13. This Figure also shows that the total pressure drop decreases with the increase of the clearance ratio. For the tested fin array configurations, going from fully shrouded to that one of largest clearance ratio ($C/H_f = 0.89$), the total pressure drop decreases from about 480 Pa to about *250 Pa*, with a percentage reduction in the total pressure drop of about *50%.*

A comparison of the heat transfer results for all fin array configurations is shown in Figure-14. For Reynolds number Re_D, of about 3200, it is seen that the average heat transfer coefficients for partially shrouded fin array of clearance ratio (C/H_f) of *0.36, 0.56,* and *0.89* compared to those of fully shrouded one are found to diminish by about *10%, 15%,* and *30%,* respectively. This reduction in the values of heat transfer coefficients becomes small as the Reynolds number increases. The improvement in the heat transfer coefficient accompanied with partially shrouded fin array of C/H_f equals to *0.22* for values of Reynolds number greater than about 7000 may be resulted from the promoted turbulence in the clearance passage which is less than the fin spacing ($C/S<1$), and that on the expense of the increased pressure drop accompanied with that configuration as noticed in Figure-13.

The fin array heat transfer response to the presence of tip-to-shroud clearance can be correlated using the collected data from the experiments. The obtained results show that the heat transfer coefficient is dependent on Reynolds number, clearance ratios C/S and C/H_f. The correlated data is presented in Figure-15 and can be expressed as

$$Nu = \frac{7.522\,\mathrm{Re}^{0.182}}{\left[(1+C/H_f)(1+C/S)\right]^{0.1096}} \qquad (23)$$

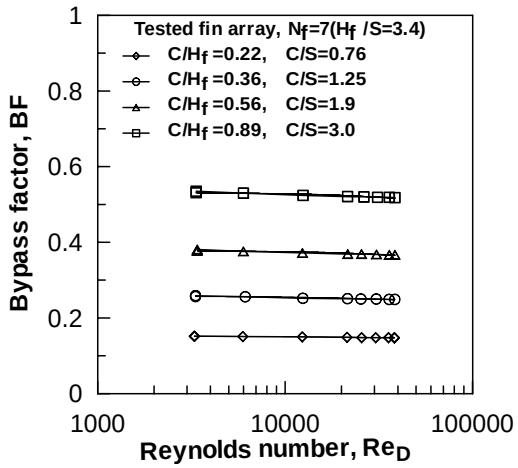

Fig. 4 Bypass factor versus Reynolds number for different tip-to-shroud clearance ratio.

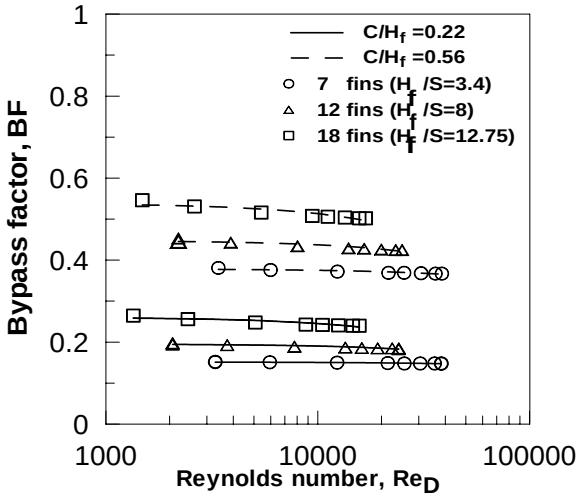

Fig.5 Bypass factor versus Reynolds number for partially-shrouded fin arrays of different fin density.

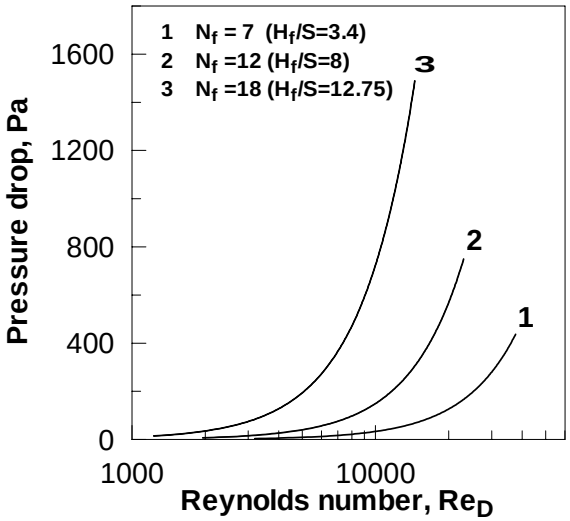

Fig.6 Total pressure drop across fully-shrouded fin array with different fin density versus Reynolds number.

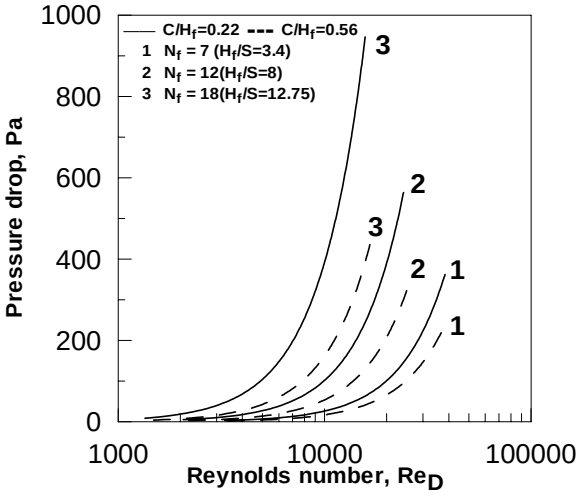

Fig. 7 Pressure drop across the fin array of different fin density versus Reynolds number at two clearance ratios.

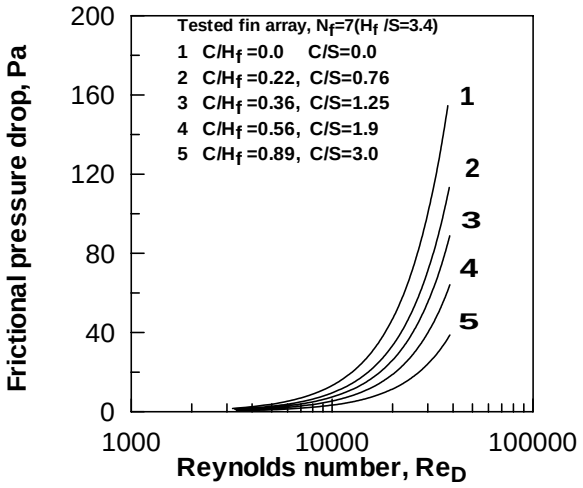

Fig. 8 Frictional pressure drop through fin passages versus Reynolds number for different clearance ratio.

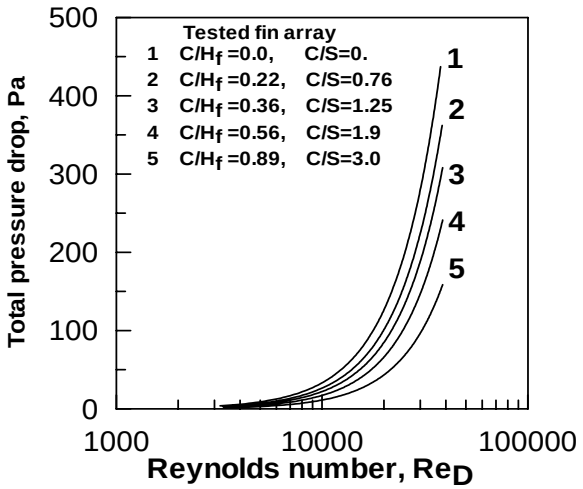

Fig. 9 Calculated pressure drop versus Reynolds number for different clearance ratio.

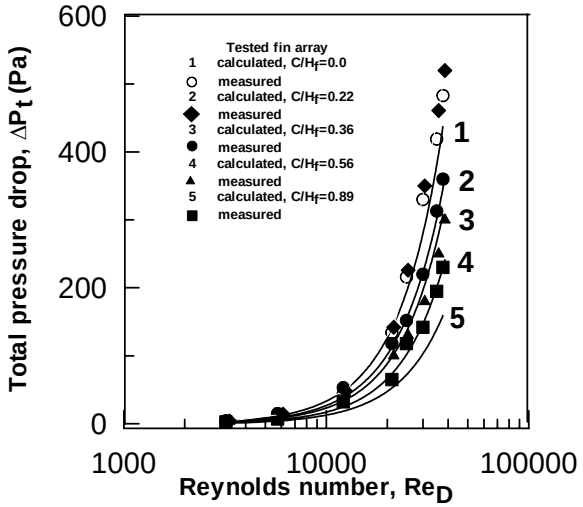

Fig. 10 Measured and calculated total pressure drop througth the tested fin array for different clearance ratio.

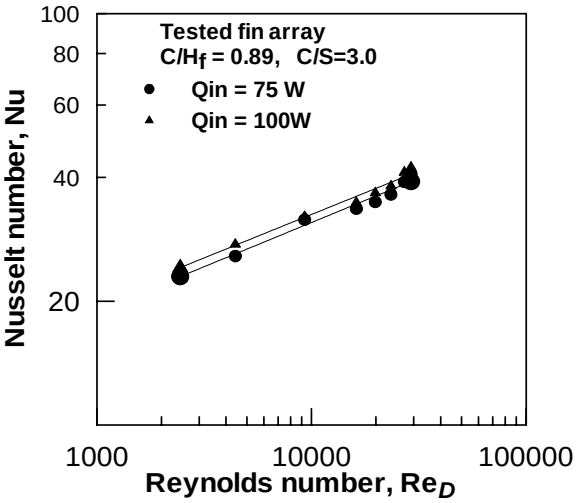

Fig.11 Nusselt number variation with Reynolds number for large clearance at two power inputs.

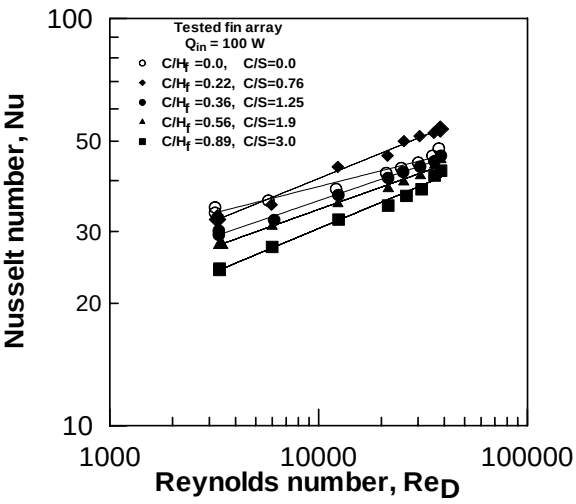

Fig. 12 Nusselt number versus Reynolds number for different tip-to-shroud clearance ratio.

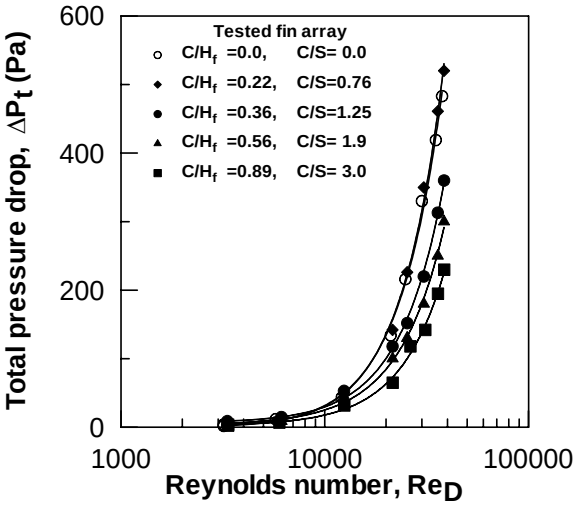

Fig.13 Measured total pressure drop versus Reynolds number for different tip-to-shroud clearance ratio.

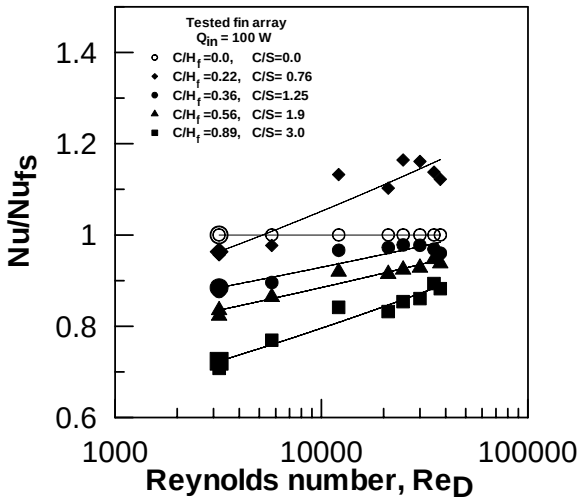

Fig. 14 Effect of tip-to-shround clearance on heat transfer performance of fully shrouded fin array.

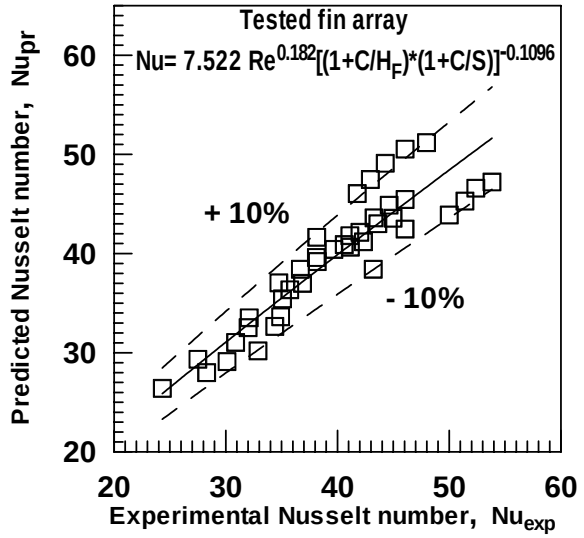

Fig.15 Correlation of the present experimental of the fin array of a horizontal base plate.

CONCLUSIONS

Experimental and theoretical analysis are carried out to investigate the effect of air velocity, and tip-to-shroud clearance on the extent of bypass factor, the pressure drop and the thermal performance of longitudinal aluminum fin arrays. The experiments were parameterized by the clearance ratios, C/H_f, C/S, and Reynolds number, Re_D. Air was the working fluid and the flow was turbulent. The following conclusions may be drawn:

a) The bypass factor increases with the increase of the clearance for all fin array configurations and is nearly constant with Reynolds number;
b) The bypass factor is greatly affected by the fin spacing. As the fin density increases the bypass factor increases tremendously;
c) The calculated total pressure drop across the fin array is magnificently increased with the decrease of fin spacing. Increasing the value of tip-to-shroud clearance, the total pressure drop across all arrays of different fin spacing decreases.
The average heat transfer coefficient for the tested fin array with the largest clearance *(C/H_f =0.89)* was less sensitive to changing power input and increased with increasing air velocity;
d) Comparing the heat transfer results corresponding to the fully and partially shrouded tested fin array, the clearance gave rise to considerable reductions in the average heat transfer coefficients. The average heat transfer coefficients for partially shrouded fin array of clearance ratio *(C/H_f)* of *0.36, 0.56,* and *0.89* compared to those of fully shrouded one were found to diminish by about *10%, 15%, and 30%,* respectively. This reduction in the values of heat transfer coefficients becomes small as the Reynolds number increases;
e) The improvement in the heat transfer coefficient accompanied with partially shrouded fin array of C/H_f equals to *0.22* may be resulted from the promoted turbulence in the clearance passage which is less than the fin spacing *($C/S<1$)* and this improvement at the expense of increased pressure drop across the array of this configuration; and
f) The obtained correlation for the heat transfer coefficient belongs to the tested fin array configurations of *$C/S>0.0$* and for air as a working fluid.

REFERENCES

Adam V. B. and Izundu F. O. 1997. Characterization of Longitudinal Fin Heat Sink - Thermal Performance and Flow Bypass Effects Through CFD Method. SEMI-THERM, Thermal and Fluid Flow Analysis Software, MAYA.

Azar K. and Tavassoli B. 2003. How Much Heat can be Extracted from a Heat Sink. Electronics Cooling. May. pp. 1-9.

Bejan A. and Sciubba E. 1992. The Optimal Spacing of Parallel Plates Cooled by Forced Convection. Int. J. Heat and Mass Transfer. 35(12): 3259- 3264.

Butterbaugh M. A. and Kang S. S. 1995. Effect of Airflow Bypass on the Performance of Heat Sinks in Electronic Cooling. ASME proceeding of Advances in Electronic Packaging. 2: 843-848.

Elshafei E. A. M. and El-Negiry E. A. 2003. Effect of Fin Configuration on the Performance of Longitudinal Fin Arrays. Mansoura Eng. Journal. 28(2): M. 57-M. 70.

Hodge B.K. 1990. Analysis and Design of Energy Systems. 2nd Edition. Prentice-Hall, Inc.

Kakac S., Shah R. K. and Aung W. 1987. Handbook of Single-Phase Convective Heat Transfer. 2nd Edition. pp. 3-42. Wiley and Sons, New York.

Kays W. M. and London A. L. 1984. Compact Heat Exchangers. 3rd Edition. pp. 108-112. McGraw Hill, Inc., New York.

Knight R. W., Hall D. J., Goodling J. S. and Jaeger R. C. 1992. Heat Sink Optimization with Application to Microchannels. IEEE. 15(5): 832-842.

Lee S. 1995. Optimum Design and Selection of Heat Sinks. IEEE Trans., CPMT-A. 18(4):

Simons R. E. 2004. Estimating the Effect of Flow Bypass on Parallel Plate-Fin Heat Sink Performance. Electronics-Cooling.com/html/, February-cc.html.

Sparrow E. M and Beckley T. J. 1981. Pressure Drop Characteristics for a Shrouded Longitudinal Fin Array with Tip Clearance. ASME Journal of Heat Transfer. 103: 393-395.

Sparrow E. M. and Kadle D. S. 1986. Effect of Tip to Shroud Clearance on Turbuleny Heat Transfer from a Shrouded, Longitudinal Fin Array. Journal of Heat Transfer. 108: 519-524.

Sparrow E. M., Baliga B. R. and Patanker S. V. 1978. Forced Convection Heat Transfer from a Shrouded Fin Array with and without Tip Clearance. ASME Journal of Heat Transfer. 100: 572-579.

Suzana P., Madhusudan I. and Avram B. 2000. Bypass Effect in High Performance Heat Sinks. Submitted to the Int. Thermal Sciences Conference in Bled, Slovenia. June 11th- 14th.

Writz R. A., Chen W. and Zhou R. 1994. Effect of Flow Bypass on the Performance of Longitudinal Fin Heat Sinks. ASME J. of Electronic Packaging. 116: 206-211.